Article

Ab Initio Studies on the Radiationless Decay Mechanisms of the Lowest Excited Singlet States of 9H-Adenine

Serhiy Perun, Andrzej L. Sobolewski, and Wolfgang Domcke

J. Am. Chem. Soc., **2005**, 127 (17), 6257-6265• DOI: 10.1021/ja044321c • Publication Date (Web): 12 April 2005

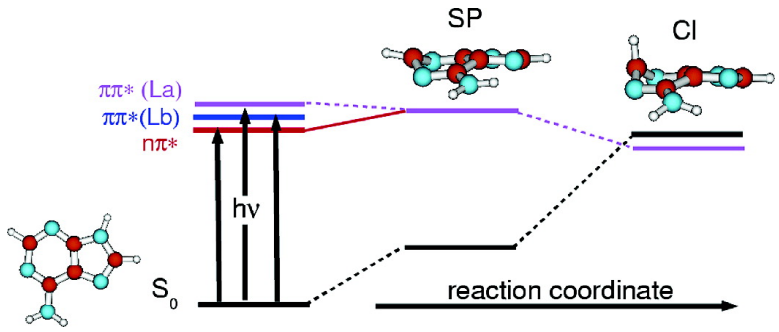

More About This Article

Additional resources and features associated with this article are available within the HTML version:

- Supporting Information
- Links to the 39 articles that cite this article, as of the time of this article download
- Access to high resolution figures
- Links to articles and content related to this article
- Copyright permission to reproduce figures and/or text from this article

View the Full Text HTML

J|A|C|S
ARTICLES
Published on Web 04/12/2005

Ab Initio Studies on the Radiationless Decay Mechanisms of the Lowest Excited Singlet States of 9H-Adenine

Serhiy Perun,[†] Andrzej L. Sobolewski,*[,†] and Wolfgang Domcke[‡]

Contribution from the Institute of Physics, Polish Academy of Sciences, PL-02668 Warsaw, Poland, and Department of Chemistry, Technical University of Munich, D-85747 Garching, Germany

Received September 17, 2004; E-mail: sobola@ifpan.edu.pl

Abstract: The mechanisms that are responsible for the rapid deactivation of the $^1n\pi^*$ and $^1\pi\pi^*$ excited singlet states of the 9H isomer of adenine have been investigated with multireference ab initio methods (complete-active-space self-consistent-field (CASSCF) method and second-order perturbation theory based on the CASSCF reference (CASPT2)). Two novel photochemical pathways, which lead to conical intersections of the S_1 excited potential-energy surface with the electronic ground-state surface, have been identified. They involve out-of-plane deformations of the six-membered aromatic ring via the twisting of the N_3C_2 and N_1C_6 bonds. These low-lying conical intersections are separated from the minimum energy of the lowest ($^1n\pi^*$) excited state in the Franck−Condon region by very low energy barriers (of the order of 0.1 eV). These properties of the S_1 and S_0 potential-energy surfaces explain the unusual laser-induced fluorescence spectrum of jet-cooled 9H-adenine, showing sharp structures only in a narrow energy interval near the origin, as well as the extreme excess-energy dependence of the lifetime of the singlet excited states. It is suggested that internal-conversion processes via conical intersections, which are accessed by out-of-plane deformation of the six-membered ring, dominate the photophysics of the lowest vibronic levels of adenine in the gas phase, while hydrogen-abstraction photochemistry driven by repulsive $^1\pi\sigma^*$ states may become competitive at higher excitation energies. These ultrafast excited-state deactivation processes provide adenine with a high degree of intrinsic photostability.

1. Introduction

The nucleic acid bases adenine, cytosine, guanine, thymine, and uracil represent some of the most important building blocks of life. The DNA and RNA bases absorb strongly in the 200−300 nm range, which renders living matter potentially vulnerable to the UV components of sunlight. The UV absorbing $^1\pi\pi^*$ excited states of the bases lie approximately 5 eV above the ground state. This significant energy deposited in the molecule by a UV photon could initiate a variety of photoreactions. Nevertheless, the quantum yields of photoproducts involving substantial rearrangements of the heteroatomic rings are very low.[1] It seems that photochemical reactions are efficiently quenched by very fast (subpicosecond) nonradiative decay processes back to the electronic ground state. These nonradiative mechanisms provide DNA with a high degree of photostability.[1−3]

The photophysical properties of adenine are typical in this respect. Resonant two-photon ionization (R2PI) and laser-induced fluorescence (LIF) spectra show sharp structures only in a narrow energy interval near the origin of the lowest $^1\pi\pi^*$ excited state.[4,5] Kang et al.[6,7] have performed pump−probe transient ionization experiments on jet-cooled bases with femtosecond laser pulses and have determined a lifetime of 1.0 ps for adenine at an excitation energy of 37 500 cm^{-1}. In aqueous solution, the transient absorption signals of adenine decay biexponentially with lifetimes of 180 ± 30 fs and 8.8 ± 1.2 ps.[8] These values agree very well with fluorescence up-conversion results of Gustavsson et al.[9] who determined lifetimes of 230 ± 50 fs and 8.0 ± 0.3 ps. The biexponentiality of the decay has a straightforward interpretation in the case of adenine: the two decay components reflect the presence of two tautomers in solution, 7H-adenine and 9H-adenine. The lifetimes of 7H-adenine and 9H-adenine differ by a factor of about 40 in aqueous solution at room temperature, despite the relatively small differences of the structures. DNA base fluorescence also was extensively studied in low-temperature glasses. The fluorescence lifetimes of various DNA bases in low-temperature environments are reported to be several nanoseconds.[10−12] This

[†] Polish Academy of Sciences.
[‡] Technical University of Munich.

(1) Cadet, J.; Vigny, P. In *Bioorganic Photochemistry*; Morrison, H., Ed.; Wiley: New York, 1990; Vol. 1, p 1.
(2) Daniels, M. In *Photochemistry and Photobiology of Nucleic Acids*; Wang, S. Y., Ed.; Academic Press: New York, 1976; Vol. 1, p 23.
(3) Crespo-Hernandez, C. E.; Cohen, B.; Hare, P. M.; Kohler, B. *Chem. Rev.* **2004**, *104*, 1977.
(4) Kim, N. J.; Jeong, G.; Kim, Y. S.; Sung, J.; Kim, S. K.; Park, Y. D. *J. Chem. Phys.* **2000**, *113*, 10051.
(5) Plützer, C.; Nir, E.; de Vries, M. S.; Kleinermanns, K. *Phys. Chem. Chem. Phys.* **2001**, *3*, 5466.
(6) Kang, H.; Jung, B.; Kim, S. K. *J. Chem. Phys.* **2003**, *118*, 6717.
(7) Kang, H.; Lee, K. T.; Jung, B.; Ko, Y. J.; Kim, S. K. *J. Am. Chem. Soc.* **2002**, *124*, 12958.
(8) Cohen, B.; Hare, P. M.; Kohler, B. *J. Am. Chem. Soc.* **2003**, *125*, 13594.
(9) Gustavsson, T.; Sharonov, A.; Onidas, D.; Markovitsi, D. *Chem. Phys. Lett.* **2002**, *356*, 49.
(10) Holmén, A.; Broo, A.; Albinsson, B.; Nordén, B. *J. Am. Chem. Soc.* **1997**, *119*, 12240.
(11) Hart, L. P.; Daniels, M. *Biochem. Biophys. Res. Commun.* **1989**, *162*, 781.

is in striking contrast to the femtosecond lifetimes observed in polar solvents at room temperature.

The isolated DNA bases exhibit an extremely excess-energy-dependent dynamics of the excited singlet states.[13,14] Optical preparation of excited states with significant vibrational excess energy leads to deactivation on a time scale of picoseconds or less, while excitation closer to the origin produces states with much longer lifetimes. Such a pronounced wavelength dependence of the lifetime has not been observed in condensed-phase environments, neither at low nor at high temperatures.[3] All of these observations indicate that specific intramolecular mechanisms must be responsible for the nonradiative decay dynamics of the DNA bases, which are, however, significantly influenced by condensed-phase environments.

It has recently been shown by several groups that the methods of ab initio quantum chemistry can contribute significantly to the identification of the specific radiationless-decay mechanisms in isolated DNA bases. Calculations on cytosine at the complete-active-space self-consistent-field (CASSCF) level led to the proposal that the $^1\pi\pi^*$ excited state decays via a conical intersection of the $^1\pi\pi^*$ state with the $^1n\pi^*$ state of the carbonyl group and a conical intersection of the latter state with the electronic ground state.[15] An alternative direct pathway via a conical intersection of the lowest $^1\pi\pi^*$ state with the electronic ground state is suggested by recent calculations at the CASPT2 (second-order perturbation theory based on the CASSCF reference) level.[16] Similar mechanisms involving out-of-plane deformation of the six-membered ring and conical intersections of the S_1 and S_0 potential-energy surfaces have been identified by CASSCF/MRCI calculations for uracil.[17] The radiationless decay of the $S_1(\pi\pi^*)$ state of 9-methylguanine has been investigated by ab initio molecular dynamics simulations.[18,19]

In addition to the commonly discussed $^1\pi\pi^*$ and $^1n\pi^*$ states, excited states of $^1\pi\sigma^*$ type, which are associated with the ubiquitous azine, amino, and enol groups, may play an essential role in the photochemistry of DNA bases. The potential-energy functions of these $^1\pi\sigma^*$ states are generically dissociative with respect to the stretching of the corresponding NH and OH bonds, and intersect not only the PE functions of the $^1\pi\pi^*$ and $^1n\pi^*$ excited states, but also that of the electronic ground state. As shown for the example of 9H-adenine by calculations using time-dependent density functional theory (TDDFT), this sequence of conical intersections may provide an alternative mechanism for the ultrafast deactivation of the excited electronic states.[20,21] Recent excited-state nonadiabatic Car−Parinello simulations on guanine in aqueous solution have provided additional evidence for the $^1\pi\sigma^*$-driven hydrogen-abstraction mechanism and its role in aqueous photoionization.[22] The existence of the $^1\pi\sigma^*$ decay mechanism has experimentally been verified by the detection of fast hydrogen atoms from the dissociation of the NH bond of 9H-adenine after excitation at 240, 243, and 266 nm in the gas phase.[23,24]

Apart from the investigation of the photochemistry of the $^1\pi\sigma^*$ states, relatively few theoretical studies have been performed on the excited-state reaction mechanisms of adenine. Vertical excitation energies of the lowest $^1\pi\pi^*$ and $^1n\pi^*$ states have been calculated with various ab initio and semiempirical methods, in particular also with multireference self-consistent-field and multireference perturbation methods.[25−29] Broo, Mennucci et al., as well as Salter and Chaban have determined equilibrium geometries of some of the excited states and have discussed the vibronic coupling of close-lying $^1\pi\pi^*$ and $^1n\pi^*$ states (the so-called proximity effect[30]) as well as the possible twisting of the amino group.[27,28]

In the present work, we have attempted a more comprehensive investigation of possible nonradiative decay channels of the lowest $^1\pi\pi^*$ and $^1n\pi^*$ states of adenine. We focus on the conical intersections of the S_1 surface with the electronic ground-state surface and the reaction paths leading from the Franck−Condon region to these conical intersections. It is nowadays well established that conical intersections are efficient funnels for the radiationless decay to the electronic ground state.[31−34] The lifetime of excited states thus is primarily determined by the barriers that separate the excited states at the Franck−Condon geometry from the low-lying conical intersections. Higher excited states, such as the $^1\pi\sigma^*$ states mentioned above, also can be connected via low-lying conical intersections with the electronic ground state. However, these intersections likely are separated by sizable potential-energy barriers from the minimum of the lowest optically accessible excited state (the $^1n\pi^*$ state in the case of adenine). In the present investigation, we focus on the nonradiative decay mechanisms with the lowest barriers, which govern the lifetime and spectroscopy near the band origin of the optical absorption spectrum.

2. Computational Details

The ground-state geometry of adenine was optimized with the restricted Hartree−Fock (RHF) second-order Møller−Plesset (MP2) method. For the geometry optimization of the excited electronic states, the CASSCF method[35] was employed. The standard 6-31G(d,p) split-valence double-ζ Gaussian basis set with polarization functions on all atoms has been used in the geometry optimizations.

The active space used for the optimization of the stationary points (local minima and saddle points) of excited states includes 12 electrons distributed over 10 valence orbitals. To locate the minimum-energy structures of the lowest $^1\pi\pi^*$ and $^1n\pi^*$ states, the geometry optimization was first performed with C_s symmetry restriction. This is the only way

(12) Polewski, K.; Zinger, D.; Trunk, J.; Monteleone, D. C.; Sutherland, J. C. *J. Photochem. Photobiol., B: Biol.* **1994**, *24*, 169.
(13) Ullrich, S.; Schultz, T.; Zgierski, M. Z.; Stolow, A. *J. Am. Chem. Soc.* **2004**, *126*, 2262.
(14) Ullrich, S.; Schultz, T.; Zgierski, M. Z.; Stolow, A. *Phys. Chem. Chem. Phys.* **2004**, *6*, 2756.
(15) Ismail, N.; Blancafort, L.; Olivucci, M.; Kohler, B.; Robb, M. A. *J. Am. Chem. Soc.* **2002**, *124*, 6818.
(16) Merchan, M.; Serrano-Andres, L. *J. Am. Chem. Soc.* **2003**, *125*, 8108.
(17) Matsika, S. *J. Phys. Chem. A* **2004**, *108*, 7584.
(18) Langer, H.; Doltsinis, N. L. *Phys. Chem. Chem. Phys.* **2003**, *5*, 4516.
(19) Langer, H.; Doltsinis, N. L. *Phys. Chem. Chem. Phys.* **2004**, *6*, 2742.
(20) Sobolewski, A. L.; Domcke, W.; Dedonder-Lardeux, C.; Jouvet, C. *Phys. Chem. Chem. Phys.* **2002**, *4*, 1093.
(21) Sobolewski, A. L.; Domcke, W. *Eur. J. Phys. D* **2002**, *20*, 369.
(22) Langer, H.; Doltsinis, N. L.; Marx, D. *ChemPhysChem*, in press.
(23) Hünig, I.; Plützer, C.; Seefeld, K. A.; Löwenich, D.; Nispel, M.; Kleinermanns, K. *ChemPhysChem* **2004**, *5*, 1427.
(24) Zierhut, M.; Roth, W.; Fischer, I. *Phys. Chem. Chem. Phys.* **2004**, *6*, 5178.
(25) Fülscher, M. P.; Serrano-Andres, L.; Roos, B. O. *J. Am. Chem. Soc.* **1997**, *119*, 6168.
(26) Broo, A.; Holmen, A. *J. Phys. Chem. A* **1997**, *101*, 3589.
(27) Broo, A. *J. Phys. Chem. A* **1998**, *102*, 526.
(28) Mennucci, B.; Toniolo, A.; Tomasi, J. *J. Phys. Chem. A* **2001**, *105*, 4749.
(29) Salter, L. M.; Chaban, G. M. *J. Phys. Chem. A* **2002**, *106*, 4521.
(30) Lim, E. C. *J. Phys. Chem.* **1986**, *90*, 6770.
(31) Xantheas, S. S.; Atchity, G. J.; Elbert, S. T.; Ruedenberg, K. *J. Chem. Phys.* **1991**, *94*, 8054.
(32) Bernardi, F.; Olivucci, M.; Robb, M. A. *Chem. Soc. Rev.* **1996**, 321.
(33) Klessinger, M.; Michl, J. *Excited States and Photochemistry of Organic Molecules*; VCH: New York, 1999.
(34) *Conical Intersections: Electronic Structure, Dynamics and Spectroscopy*; Domcke, W., Yarkony, D. R., Köppel, H., Eds.; World Scientific: Singapore, 2004.
(35) Roos, B. O. *Adv. Chem. Phys.* **1987**, *69*, 399.

to distinguish between the a″(π) and a′(σ/n) orbitals and to divide the electronically excited states into blocks of A′ and A″ symmetry. For the geometry optimization of the $^1\pi\pi^*$ state, the active space consisted of 10 orbitals of π character. This active space was modified by replacing the lowest-energy π orbital by a lone-pair orbital (n) for the calculation of the equilibrium structure of the $^1n\pi^*$ state. Taking the local minimum structures of the $^1\pi\pi^*$ and $^1n\pi^*$ states, which were obtained with C_s constrained optimization, and the respective sets of canonical orbitals as initial guesses, we relaxed the symmetry constraint and reoptimized the geometry of the respective states in C_1 symmetry. The search for nonplanar saddle-point structures was performed with an active space consisting of nine orbitals, which are nominally of π character, and one orbital of n character, with no symmetry constraints imposed. The nature of the stationary points was checked by calculating the Hessian matrix and analyzing the harmonic frequencies. These calculations were carried out with the GAMESS program package.[36]

The search for conical intersections between the ground state and the lowest excited singlet state was performed with the method which is implemented in the Gaussian 98 program package.[37] Due to internal limitations of this program, the active space for the CASSCF calculations had to be reduced to 6 electrons distributed in 6 orbitals. The active space was constructed from the three HOMOs and the three LUMOs obtained from a RHF calculation performed at the guessed geometry of the conical intersection. The guessed geometries of the conical intersections were constructed by stretching and twisting one of the two C−N bonds of the six-membered ring of adenine. The conjecture that this kind of deformation may lead to the intersection of the S_1 and S_0 surfaces is based on our previous experience gained in the study of benzene and pyrazine[38] and the guanine−cytosine base pair.[39]

Having optimized the local minima of the excited states and the conical intersections, a linearly interpolated internal-coordinate (LIIC) reaction path was constructed. The LIIC path is defined as the straight line in the multidimensional internal-coordinate space, which connects a given initial local minimum with a given conical intersection. Single-point energy calculations have been performed along each LIIC path to obtain the reaction-path potential-energy profiles. These single-point energy calculations were performed with the MOLCAS-4 package[40] using the ANO-L (3s2p1d/2s1p) split-valence double-ζ basis set with polarization functions on all atoms. The active space consisted of 12 electrons in 10 orbitals. The six lowest electronic states were included in the CASSCF energy functional with equal weights.

The continuity of the character of the excited states along a given reaction path was controlled by the calculation of the transition dipole moments from the ground state to the corresponding excited state as well as by the analysis of the electronic configurations composing the CASSCF wave functions. The molecular geometry corresponding to the maximum of the potential-energy profile of the lowest excited singlet state along a given LIIC reaction path was used as the initial guess for the search of the saddle point of this path.

Finally, single-point energy calculations were performed at the optimized ground-state geometry as well as at the excited-state local minima, saddle points, and conical-intersection structures with the CASPT2 method.[41] The underlying CASSCF wave functions were obtained by a state-averaged CASSCF calculation, including the three lowest states with equal weights in the energy functional. To mitigate the effect of intruder states in the CASPT2 calculations, a level-shift technique, the so-called LS-CASPT2 approach,[40] with an imaginary shift of 0.3 au was used. To calculate the oscillator strength of optical transitions, the CASSCF transition dipole moments were combined with excitation energies obtained by the CASPT2 method.

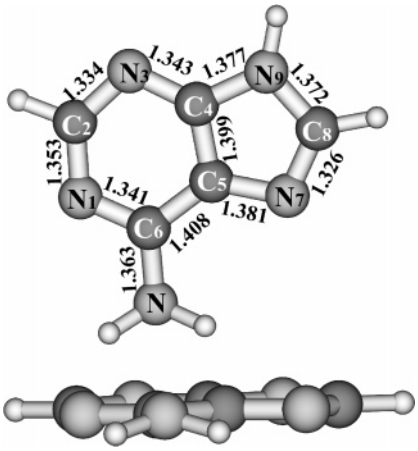

Figure 1. Ground-state equilibrium geometry of 9H-adenine (top and side views) determined at the MP2/6-31G(d p) level. Bond lengths are given in angstroms.

3. Results and Discussion

3.1. Ground-State Geometry. The MP2/6-31G(d,p)-optimized ground-state geometry of 9H-adenine is shown in Figure 1. The Cartesian geometry parameters of this structure as well as of the other structures optimized in this work are given in the Supporting Information.

The resulting structure is almost planar, with a slightly pyramidized amino group (the relevant dihedral angles are $\delta(N_1C_6NH) = 18.3°$ and $\delta(C_5C_6NH) = -20.6°$). The breaking of the C_s symmetry results in a stabilization of the energy by 0.3 kcal/mol. The optimized bond lengths, bond angles, and dihedral angles agree reasonably well with previous experimental[42] and theoretical[43−46] findings. The computed dipole moment of the ground state is 2.71 D at this level of theory. It compares well with experimental results for crystalline 9-methyladenine[47] (2.4 D) and for 9-butyladenine in solution[48] (3.0 ± 0.2 D) as well as with theoretically determined values.[25]

3.2. Vertical Excitation Energies. The CASSCF/CASPT2 vertical excitation energies, oscillator strengths, and dipole moments of the five lowest excited states of adenine are given in Table 1.

It should be noted that the inclusion of dynamical electron correlation changes the ordering and the spacing of the excited states. The CASPT2 method predicts that the two close-lying states of $^1\pi\pi^*$ character (^1L_b and ^1L_a, respectively) are followed by the $^1n\pi^*$ state, while the ^1L_a state is considerably higher in energy at the CASSCF level. Inclusion of dynamical electron correlation effects thus is essential for a quantitatively accurate description of the excitation spectrum of 9H-adenine.

(36) Schmidt, M. W.; Baldridge, K. K.; Boatz, J. A.; Elbert, S. T.; Gordon, M. S.; Jensen, J. H.; Koseki, S.; Matsunaga, M.; Nguyen, K. A.; Su, S. J.; Windus, T. L.; Dupuis, M.; Montgomery, J. A. *J. Comput. Chem.* **1993**, *14*, 1347.
(37) Frisch, M. J.; et al. *Gaussian 98*; Gaussian, Inc.: Pittsburgh, PA, 1998.
(38) Sobolewski, A. L.; Woywod, C.; Domcke, W. *J. Chem. Phys.* **1993**, *98*, 5627.
(39) Sobolewski, A. L.; Domcke, W. *Phys. Chem. Chem. Phys.* **2004**, *6*, 2763.
(40) Andersson, K.; et al. *MOLCAS, Version 4, User's Guide*; University of Lund, Sweden, 1997.
(41) Roos, B. O.; Andersson, K. *Chem. Phys. Lett.* **1995**, *245*, 215.
(42) McMullan, R. K.; Benci, P.; Craven, B. M. *Acta Crystallogr., Sect. B* **1980**, *36*, 1424.
(43) Broo, A.; Holmen, A. *Chem. Phys.* **1996**, *211*, 147.
(44) Jean, J. M.; Hall, K. B. *J. Phys. Chem. A* **2000**, *104*, 1937.
(45) Sponer, J.; Florian, J.; Hobza, P.; Leszczynski, J. *J. Biomol. Struct.* **1996**, *13*, 827.
(46) Chandra, A. K.; Nguyen, M. T.; Uchimaru, T.; Zeegers-Hyskens, T. *J Phys. Chem. A* **1999**, *103*, 8853.
(47) Eisenstein, M. *Acta Crystallogr.* **1988**, *B44*, 412.
(48) De Voe, H.; Tinoco, I., Jr. *J. Mol. Biol.* **1962**, *4*, 500.

Table 1. CASSCF and CASPT2 Vertical Excitation Energies, Dipole Moments (μ), and Oscillator Strengths (f) of the Excited States of 9H-Adenine Computed at the MP2/6-31G(d,p) Ground-State Equilibrium Geometry of C_1 Symmetry

state	E (CASSCF), eV	E (CASPT2), eV	μ, D	f
S_1 $^1\pi\pi^*$ (^1L_b)	5.226	4.852	2.700	0.0064
S_2 $^1\pi\pi^*$ (^1L_a)	6.859	4.902	4.653	0.1416
S_3 $^1n\pi^*$	6.193	5.503	1.628	0.0039
S_4 $^1n\pi^*$	6.674	5.685	1.622	0.0061
S_5 $^1\pi\pi^*$	7.232	6.098	1.203	0.0374

While the ground state and the ^1L_b and $^1n\pi^*$ states are relatively unpolar, the dipole moment of the ^1L_a state is significant (4.7 D). Thus, a significant solvatochromic shift is expected for the ^1L_a state in polar solvents.

Table 1 shows that the CASPT2 vertical excitation energy of the lowest $^1n\pi^*$ state of adenine is about 0.7 eV higher than that of the ^1L_b state. This result is significantly different from TDDFT and CIPSI results,[28] which predicted the lowest $^1\pi\pi^*$ and $^1n\pi^*$ vertical excitation energies to be essentially equal. The TDDFT vertical excitation energy of the lowest $^1n\pi^*$ state, but not the energy of the ^1L_b state, compares well with the CASPT2 results.

The CASPT2 energies of the first two $^1\pi\pi^*$ vertical transitions calculated at the nonplanar ground-state equilibrium geometry agree very well with the UV/vis absorption spectrum of adenine in the gas phase,[49] which exhibits a low-energy band peaking at 252 nm (4.92 eV). The vertical excitation energy of the first $^1n\pi^*$ excited state, 5.5 eV, can be compared to an CD experiment on adenosine,[50] where a band at 230 nm (5.4 eV) has been assigned as the lowest $^1n\pi^*$ transition.

3.3. Excited-State Minimum-Energy Structures and Energetics. The CASSCF equilibrium geometries of the $^1\pi\pi^*$(^1L_b) state and the lowest $^1n\pi^*$ state are shown in Figure 2a and b, respectively (see also Supporting Information). The Hessian matrices calculated at the stationary points confirm that they represent true minima of the S_1 potential-energy surface.

The nonplanarity of the minimum geometry of the ^1L_b state is essentially confined to the pyramidization of the amino group, which is slightly more pronounced than in the ground state. The respective dihedral angles are $\delta(N_1C_6NH) = 22.4°$ and $\delta(C_5C_6NH) = -21.3°$. Broo[27] has found a significant out-of-plane deformation of the five-membered ring for the optimized geometry of the lowest $^1\pi\pi^*$ state, obtained with the AM1-CI(4/4) and CASSCF(4/4)/6-31G methods. At the present level of electronic-structure theory, we can conclude that the minimum geometry of the ^1L_b state is almost planar with the exception of the amino group.

The equilibrium structure of the lowest $^1n\pi^*$ excited state (Figure 2b) exhibits, in addition to the pyramidization of amino group with respective angles $\delta(N_1C_6NH) = -19.3°$ and $\delta(C_5C_6NH) = 19.1°$, a significant out-of-plane deformation of the six-membered ring, in particular for the $N_1C_2N_3$ moiety with $\delta(C_6N_1C_2H) = 172.4°$ and $\delta(C_6N_1C_2N_3) = 34.6°$. The $^1n\pi^*$ equilibrium geometry determined in the present work is in qualitative agreement with that obtained by Broo[27] at the CIS/6-31G level. The out-of-plane distortion of the $^1n\pi^*$ equilibrium geometry is the result of vibronic coupling of the $^1n\pi^*$ state with the higher-lying $^1\pi\pi^*$ states via out-of-plane coupling modes.

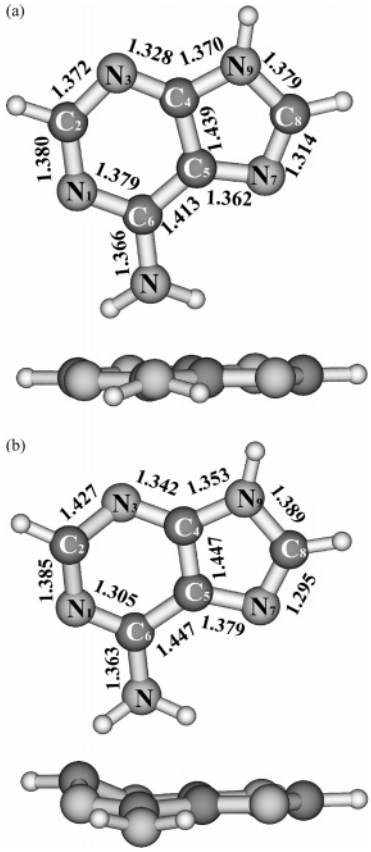

Figure 2. CASSCF equilibrium geometry of the $^1\pi\pi^*$(^1L_b) state (a) and $^1n\pi^*$ state (b) of 9H-adenine (top and side views). Bond lengths are given in angstroms.

Table 2. CASSCF and CASPT2 0−0 Excitation Energies, Dipole Moments (μ), and Oscillator Strengths (f) of the Lowest $^1n\pi^*$ and $^1\pi\pi^*$ (^1L_b) Excited States of 9H-Adenine Computed at the Respective CASSCF Optimized Excited-State Geometries

state	E (CASSCF), eV	E (CASPT2), eV	E exp,[a] eV	μ, D	f
$^1n\pi^*$	5.175	4.476	4.40	2.776	0.0035
$^1\pi\pi^*$ (^1L_b)	5.149	4.685	4.48	2.461	0.0057

[a] R2PI spectroscopy of jet-cooled adenine.[4]

The CASPT2 0−0 transition energies, the dipole moments, and the oscillator strengths of the lowest $^1n\pi^*$ state and the $^1\pi\pi^*$(^1L_b) state of 9H-adenine, calculated at the corresponding CASSCF minimum geometries, are given in Table 2.

The difference of the two 0−0 excitation energies (without correction for the zero-point vibrational energy) is 0.21 eV according to the present calculation. The results of a R2PI spectroscopy experiment on adenine[4] are given in Table 2 for comparison. These authors have assigned the lines at 4.40 and 4.48 eV to the 0−0 bands of the $^1n\pi^*$ and $^1\pi\pi^*$ transitions, respectively. The positions of the lines and the gap of 0.08 eV between them agree with the CASPT2 results within the expected precision of the method, supporting the assignments of the R2PI spectra.[4,5]

Several authors have previously reported calculated 0−0 excitation energies of 9H-adenine. Sobolewski and Domcke[21] obtained 0−0 excitation energies of 4.75 and 5.05 eV for the lowest $^1n\pi^*$ and $^1\pi\pi^*$ states, respectively, at the TDDFT level. With the CIPSI method, combined with CIS geometry optimization, 0−0 excitation energies of 3.77 and 4.71 eV were obtained

(49) Clark, L. B.; Peschel, G. G.; Tinoco, I., Jr. *J. Phys. Chem.* **1965**, *69*, 3615.
(50) Sprecher, C. A.; Johnson, W. C., Jr. *Biopolymers* **1977**, *16*, 2243.

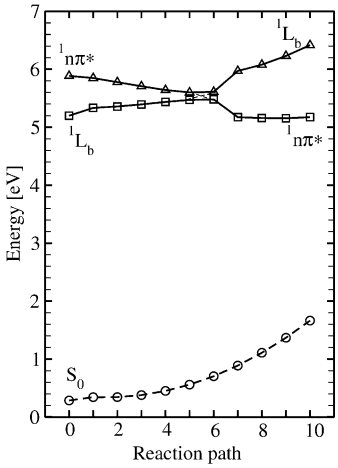

Figure 3. CASSCF potential-energy profiles of the ground state (○), the S_1 state (□), and the S_2 state (△) of 9H-adenine along the LIIC reaction path from the equilibrium geometry of the ^1L_b state to the equilibrium geometry of the $^1n\pi^*$ state.

for the $^1n\pi^*$ and $^1\pi\pi^*$ states.[28] Broo[27] predicted the band maxima of the $^1n\pi^*\rightarrow S_0$ and $^1\pi\pi^*\rightarrow S_0$ fluorescence transitions at 3.32 and 4.02 eV, respectively. It seems that these earlier calculations have overestimated the difference of the 0−0 transition energies of the $^1n\pi^*$ and ^1L_b states.

It has been noted previously by several authors that the ordering of the lowest $^1n\pi^*$ state and the $^1\pi\pi^*(^1L_b)$ state of adenine is reversed by the excited-state geometry optimization: while the $^1n\pi^*$ state lies above the ^1L_b state at the ground-state equilibrium geometry, it becomes the lowest excited state upon geometry optimization. The CASSCF adiabatic potential-energy profiles of the ^1L_b and $^1n\pi^*$ states along the LIIC reaction path connecting the equilibrium geometries of the two states are shown in Figure 3.

One can see that each of the states is the lowest excited singlet state at its own equilibrium geometry. The potential-energy functions cross (or avoid crossing) near the middle of the reaction path. At this point, the wave functions of the two states are strongly mixed, having nearly equal $n\pi^*$ and $\pi\pi^*$ character. The dashed lines in Figure 3 have been drawn as a guide for the eye to indicate the diabatic connection of the potential-energy functions based on the analysis of the wave functions. The adiabatic PE profiles are so flat and the states are so strongly mixed that it was impossible to locate (at the CASSCF level) the saddle point that separates the minima of the states. The barrier is probably very low. Broo,[27] for instance, has reported a value of 0.14 kcal/mol for this barrier height. Another interesting aspect of the potential-energy functions shown in Figure 3 is the significant increase of the energy of the ground state along the reaction path from the ^1L_b minimum to that of the $^1n\pi^*$ state. This reflects the magnitude of the geometry changes upon electronic excitation. These changes are more pronounced for the $^1n\pi^*$ state than for the ^1L_b state. Note, however, that the $^1n\pi^*-S_0$ energy gap remains significant (>3.5 eV) at the $^1n\pi^*$ equilibrium geometry. The often cited proximity effect[30] (flattening of the $^1n\pi^*$ surface by vibronic coupling with nearby $^1\pi\pi^*$ states) thus cannot explain a rapid depopulation of the $^1n\pi^*$ state via internal conversion to the electronic ground state.

Optimization of the minimum of the seam of conical intersection between the ^1L_b and $^1n\pi^*$ states at the CASSCF level was successful and has led to the structure shown in Figure 4.

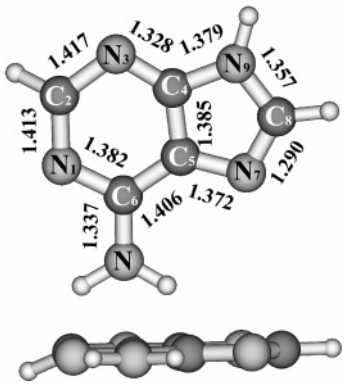

Figure 4. CASSCF optimized geometry of the conical intersection of the ^1L_b and $^1n\pi^*$ excited states of 9H-adenine (top and side views). Bond lengths are given in angstroms.

The obtained geometry is nearly planar, with the exception of the out-of-plane displacement of the CH group at the C_2 atom. The respective dihedral angles are $\delta(C_6N_1C_2H) = 156.9°$ and $\delta(C_6N_1C_2N_3) = 2.2°$. It is interesting that the amino group of this conical-intersection structure is almost planar, with dihedrals $\delta(N_1C_6NH) = -3.8°$ and $\delta(C_5C_6NH) = 2.5°$, whereas it is pyramidized at the equilibrium geometries of the S_0, ^1L_b, and $^1n\pi^*$ states. The $^1\pi\pi^*-^1n\pi^*$ conical-intersection geometry is not very different from the equilibrium geometry of the $^1\pi\pi^*(L_b)$ state and thus should be easily accessible after optical excitation of the latter. This supports the conclusion that the spectra of the lowest $^1\pi\pi^*$ and $^1n\pi^*$ states of adenine are strongly vibronically mixed.[3−8,13,14]

3.4. S_0-S_1 Conical Intersections and Correlation Diagrams. Previous calculations on the DNA bases cytosine,[15,16] uracil,[17,51] and the guanine−cytosine base pair[39] have revealed the existence of S_0-S_1 conical intersections induced by out-of-plane deformations of the six-membered ring. It has been argued in ref 39 that the out-of-plane distortion arises from the twisting of C−C or C−N bonds of the six-membered ring, analogous to phenomena that have previously been discussed for benzene and pyrazine.[38,52,53]

The six-membered aromatic ring of adenine consists of four carbon and two nitrogen atoms, which form three nominal double bonds in the ground state. Because the ring-fusing C_4-C_5 bond can be expected to be rigid with respect to out-of-plane deformation, the two C−N bonds and the C_5-C_6 bond are the primary candidates for twisting. Assuming that the twisting of the N−C bonds in adenine has a similar influence on the energetics of the S_0 and S_1 states as the distortion of the C═C bond of cytosine,[39] we have deformed the six-membered ring of adenine correspondingly and have performed unconstrained CASSCF optimizations of S_0-S_1 conical intersections. When the optimization was started with a twisted N_3C_2 bond, the structure shown in Figure 5a was obtained, henceforth referred to as CI_{32}. Predeformation of the N_1C_6 bond resulted in the structure shown in Figure 5b, referred to as CI_{16} in what follows.

(51) Shukla, M. K.; Mishra, P. C. *Chem. Phys.* **1999**, *240*, 319.
(52) Kato, S. *J. Chem. Phys.* **1988**, *88*, 3045.
(53) Palmer, I. I.; Ragazos, I. N.; Bernardi, F.; Olivucci, M.; Robb, M. A. *J. Am. Chem. Soc.* **1992**, *114*, 673.

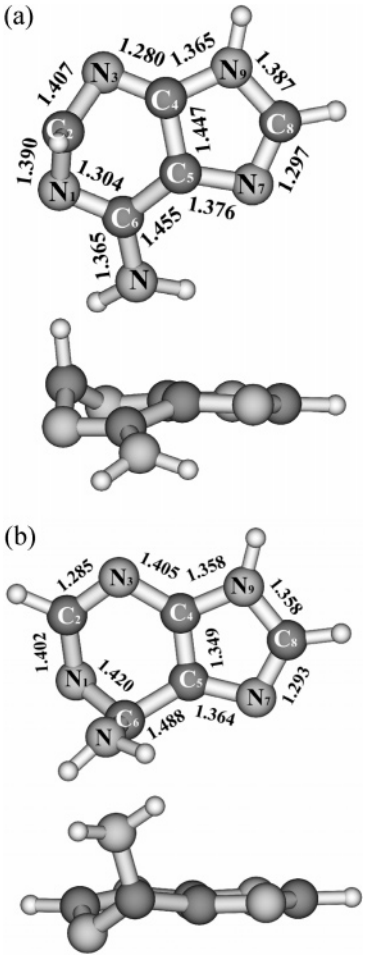

Figure 5. CASSCF optimized geometries of the conical intersections of the S_0 and S_1 states of 9H-adenine (top and side views). (a) CI_{32} is associated with the torsion of the N_3C_2 bond. (b) CI_{16} is associated with the torsion of the N_1C_6 bond. Bond lengths are given in angstroms.

Both structures are strongly nonplanar (see also Supporting Information). Comparing the CI_{32} structure (Figure 5a) with the minimum-energy structure of the $^1n\pi^*$ state (Figure 2b), one can notice a certain similarity. The CI_{32} structure can be considered to be an extrapolation of the out-of-plane deformation of the $N_1C_2N_3$ part of the six-membered ring of the $^1n\pi^*$ minimum. The dihedral angle $\delta(C_6N_1C_2N_3) = 67.6°$ of the CI_{32} structure is approximately 2 times larger than the corresponding angle at the $^1n\pi^*$ minimum. The other characteristic dihedral angle, $\delta(C_6N_1C_2H) = -84.1°$, is a similar extrapolation of $\delta(C_6N_1C_2H) = 172.4°$ of the $^1n\pi^*$ minimum structure.

Because the CI_{16} structure is related to the torsion of the N_1C_6 bond, the structural parameters that describe this deformation are the dihedral angles $\delta(C_2N_1C_6N_6) = 66.0°$ and $\delta(C_6N_1C_2H) = -142.3°$. The very similar values of about 65° of the $\delta(C_2N_1C_6N_6)$ and $\delta(C_6N_1C_2N_3)$ dihedral angles, which characterize the twisting of the N_1C_6 and N_3C_2 bonds, respectively, of the two conical intersections, indicate that S_1-S_0 degeneracy induced by C−N bond twisting of about 65° may be a general property of six-membered aromatic and heteroaromatic rings. Dihedral angles of about 59° and 65° were determined for the S_1-S_0 conical intersections of cytosine[15,16] and uracil,[17] respectively.

The knowledge of the approximate geometry and energy of the S_1-S_0 conical intersections allows us to discuss key aspects

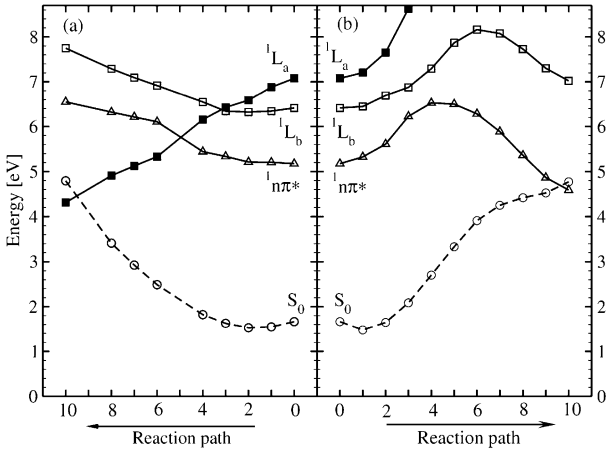

Figure 6. CASSCF potential-energy profiles of the ground-state S_0 (○), the $^1n\pi^*$ state (△), the ^1L_b state (□), and the ^1L_a state (■) of 9H-adenine along the LIIC reaction path from the equilibrium geometry of the $^1n\pi^*$ state to the CI_{32} (a) and CI_{16} (b) conical intersections. The diabatic correlation of the states is shown in (a).

of the topography and diabatic connectivity of the excited-state potential-energy surfaces. From the photophysical point of view, the most crucial aspect is the accessibility of the low-lying S_1-S_0 conical intersections from the Franck−Condon region of the lowest excited singlet state.[32−34] The existence of S_1-S_0 conical intersections itself does not guarantee effective internal conversion to the ground state, because the access of the excited-state wave packet to the conical intersections may be inhibited by barriers. To explore this aspect of the excited-state potential-energy surfaces, we have constructed CASSCF correlation diagrams of the lowest $^1n\pi^*$ state and the $^1\pi\pi^*(L_b)$ and $^1\pi\pi^*(L_a)$ states as well as the ground state along the LIIC reaction paths leading from the minimum of the $S_1(n\pi^*)$ state to the CI_{32} and CI_{16} structures, respectively. The corresponding CASSCF reaction-path energy profiles are shown in Figure 6a and b, respectively. They were constructed as described in section 2. We emphasize that these LIIC/CASSCF potential-energy functions are intended to give a qualitative overview of the diabatic state correlations. They do not provide quantitative energetic information, because (i) the reaction paths are not minimum-energy paths and (ii) dynamical electron-correlation effects are lacking.

Figure 6 reveals interesting differences of the potential-energy profiles along the two reaction paths. For the CI_{32} reaction path, the potential-energy functions of both the $^1n\pi^*$ and the ^1L_b states increase, while the energy of the diabatic ^1L_a state steeply decreases, thereby intersecting the ^1L_b, $^1n\pi^*$, and S_0 potential functions (see Figure 6a). From the point of view of photophysics, the most interesting intersections are the $^1L_a-S_0$ and $^1L_a-{}^1n\pi^*$ crossings. While the former intersection provides an efficient mechanism for radiationless relaxation to the ground state, the latter creates a barrier on the adiabatic S_1 potential-energy surface, which separates the minimum of the S_1 surface from the S_0-S_1 crossing seam.

We have determined the geometric structure of this saddle point (henceforth referred to as SP_1) at the CASSCF level. It is shown in Figure 7a. The structure is nonplanar and resembles the $^1n\pi^*$ minimum and CI_{32} structure, with characteristic dihedral angles $\delta(C_6N_1C_2N_3) = 48.1°$ and $\delta(C_6N_1C_2H) = -139.1°$. The normal-mode analysis at the SP_1 geometry shows

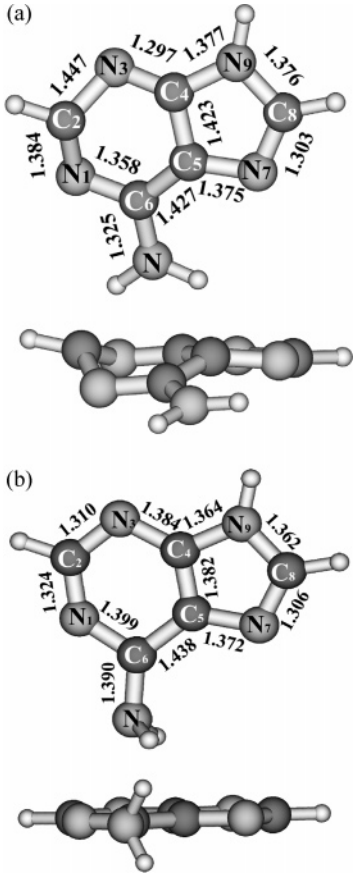

Figure 7. CASSCF optimized geometries of the saddle points on the adiabatic potential-energy surface of the first excited state of adenine (top and side views): (a) structure of SP_1, (b) structure of SP_2. Bond lengths are given in angstroms.

that only one imaginary vibrational frequency (of 167 cm^{-1}) exists in this case, confirming a first-order saddle point.

The energy profiles of the reaction path leading from the minimum of the $^1n\pi^*$ state to the CI_{16} conical intersection are shown in Figure 6b. In this case, the potential-energy functions of the $^1n\pi^*$, ^1L_b, and ^1L_a excited states exhibit relatively high barriers, which are, however, a consequence of the fact that the reaction path is not a minimum-energy reaction path. It should be noted that the CI_{16} intersection represents a $^1n\pi^*-S_0$ crossing; that is, the S_1 state has $n\pi^*$ character in the vicinity of the crossing. The $^1n\pi^*$ energy profile indicates that there should exist a saddle point on the potential-energy surface of $^1n\pi^*$ state that separates the $^1n\pi^*$ minimum from CI_{16}. The geometry optimization at the CASSCF level led to the structure shown in Figure 7b, referrred to as SP_2 in the following. The nonplanarity of the SP_2 geometry is confined to the rotation of the amino group, which is twisted by about 90° in comparison with the $^1n\pi^*$ equilibrium geometry. The vibrational analysis of the SP_2 structure shows the presence of only one imaginary frequency (of 344 cm^{-1}), which corresponds to the vibration of the amino group with respect to the ring plane. The geometry of the saddle point indicates that the minimum-energy reaction path connecting the minimum of the $^1n\pi^*$ state with the CI_{16} conical intersection is strongly curved in the space of internal coordinates. The passage from the $^1n\pi^*$ minimum to SP_2 involves mostly the rotation of the amino group, while the geometric relaxation after the saddle point mainly consists of out-of-plane wagging of this group.

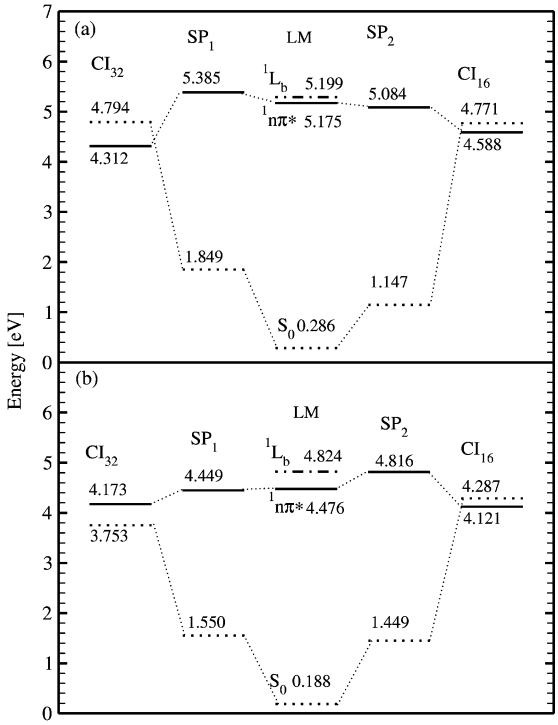

Figure 8. CASSCF (a) and CASPT2 (b) energy level diagrams of the S_0 (dotted line) and S_1 (solid line) states of 9H-adenine, computed at the geometry of the local minimum (LM) of the $^1n\pi^*$ state, at the saddle points (SP_1, SP_2) of the S_1 potential-energy surface and at the S_0-S_1 conical intersections (CI_{32}, CI_{16}). The dashed−dotted line indicates the minimum energy of the $S_2(^1L_b)$ excited state. The energies are given in electronvolts relative to the minimum energy of the ground state.

An interesting question concerns the electronic-structure mechanisms that are responsible for the CI_{32} and CI_{16} conical intersections. The two conical intersections can be assigned as arising from $^1\pi\pi^*(L_a)-S_0$ and $^1n\pi^*-S_0$ diabatic state crossings, respectively, as discussed above. Although the analysis of the wave functions in terms of molecular orbitals is not straightforward for such strongly out-of-plane distorted geometries, it is instructive to analyze the energies of the molecular orbitals that are involved in the lowest electronic transitions. In the Supporting Information, the energies of the two highest occupied and two lowest unoccupied (with respect to the HF reference) canonical CASSCF orbitals are shown as a function of the two LIIC paths. Analysis of the frontier orbitals along the CI_{32} reaction path shows that these orbital energies remain well separated from each other, implying that the orbitals can be considered to change adiabatically along this reaction path. Along the CI_{16} reaction path, on the other hand, the two HOMOs as well as the two LUMOs exhibit an avoided crossing along the path. The decrease of the S_1 energy after passing the barrier results from the steep decrease of the energy of the second π^* orbital. It can be concluded that the two conical intersections of the S_1 surface with the ground-state surface determined in this work reflect properties of the π-electronic system, or more precisely, the nodal structure of the two lowest π^* orbitals. The n orbital comes into play only insofar as the nonplanarity of the system does not allow a strict separation of n and π orbitals.

Our final results on the energetics of local minima, saddle points, and conical intersections of the excited states of 9H-adenine are given in Figure 8, which shows the CASSCF (a) and CASPT2 (b) energies obtained by single-point energy

calculations at the CASSCF-determined geometries discussed above. Energies of the S_1 surface are shown as full lines, and energies of the S_0 surface are shown as dashed lines. The dashed−dotted lines in Figure 8 represent the minimum energy of the $S_2(^1L_b)$ state. It can be seen that the energies calculated for the S_0 and S_1 states at the CI_{32} and CI_{16} geometries do not truly coincide. This reflects the fact that the geometries of the conical intersections have been determined at a lower computational level (CASSCF with a 6/6 active space) than the single-point energy calculations. These deviations are a measure of the accuracy of the present calculations. The mean values of the S_0 and S_1 energies of CI_{32} and CI_{16} given in Figure 8a (8b) are our best estimates for the energies of these conical intersections at the CASSCF (CASPT2) level. At both computational levels, it is found that both S_1-S_0 conical intersections lie below the minimum energy of the lowest excited state in the Franck−Condon region. Both conical intersections thus are energetically accessible from the optically prepared excited states.

The lifetime of the vibronic levels near the band origin is governed by the two barriers (SP_1, SP_2), which separate the Franck−Condon geometry from the two S_1-S_0 conical intersections. These conical intersections can efficiently quench the population of the S_1 state if the energy of excitation is high enough to overcome the lowest barrier. The CASSCF energies calculated at the SP_1 and SP_2 geometries are 0.21 eV higher and 0.09 eV lower, respectively, than the CASSCF energy of the equilibrium geometry of the $^1n\pi^*$ state. The situation is reversed at the CASPT2 level: now the energy calculated at the SP_1 geometry is 0.03 eV lower than the CASPT2 energy of the $^1n\pi^*$ equilibrium geometry, while the CASPT2 energy at the SP_2 geometry is 0.34 eV higher. This result implies that the saddle-point SP_1 does not exist at all at the CASPT2 level. One has to keep in mind, however, the approximate character of these results. First, the stationary points determined at the CASSCF level are not true stationary points of the CASPT2 surface. Second, the expected errors of the CASPT2 method are of the order of a few tenths of an electronvolt. Our results thus are fully consistent with two low barriers of the order of 0.1 eV, which protect the lowest vibronic levels of the $^1n\pi^*$ and ^1L_b states from the S_1-S_0 conical intersections.

3.5. Discussion of the Photophysics. The qualitative model of the photophysical dynamics of the lowest excited singlet states of 9H-adenine, which emerges from our calculations, is in full accord with the results of recent R2PI and LIF experiments on jet-cooled adenine.[4,5,54,55] The calculated (CASPT2) 0−0 energies of the $^1n\pi^*$ state and the ^1L_b state support the experimental assignments in refs 4, 5. Moreover, the very short progression of sharp vibronic lines, extending over only 0.1 eV and followed by a sharp cutoff of the fluorescence, which is a characteristic feature of the LIF spectrum of adenine,[4,5] is qualitatively explained by the existence of two very low barriers that separate the $^1n\pi^*$ and ^1L_b minima from the conical intersections with the ground state (CI_{32} and CI_{16}, see Figure 8b). For a more quantitative determination of these barriers, more accurate electronic-structure calculations, for example, with MRCI methods, and with a consistent geometry optimization of the saddle points have to be performed.

The significant excitation-energy dependence of the excited-state lifetime of adenine is another effect that can be understood on the basis of the present results. Ullrich et al.[13,14] concluded, based on femtosecond time-resolved photoelectron spectroscopy studies, that excitation of adenine at 267 or 250 nm populates the optically bright $^1\pi\pi^*(L_b)$ singlet state, which decays in less than 50 fs to the lowest $^1n\pi^*$ state. They suggested that the latter state subsequently decays to S_0 in 750 fs. Excitation closer to the origin, at 277 nm, resulted in a lifetime of several picoseconds, which was attributed by the authors to decay via intersystem crossing. In our opinion, the reason for this unusual dynamical behavior is the property of the ^1L_a excited state indicated in Figure 6a: the energy profile of this state is repulsive along the CI_{32} reaction path and crosses the energies of all lower singlet states. This state, which is the second state in the vertical absorption spectrum, with a calculated (CASPT2) energy of 4.9 eV (253 nm), is the most strongly allowed state for optical excitation from the ground state among the first five excited states and thus dominates the first absorption band of adenine. The absence of a barrier that separates the vertically excited ^1L_a state from the CI_{32} conical intersection suggests an extremely short lifetime of this state. These observations explain the results of Ullrich et al.,[13,14] because excitation at 250 nm should populate directly the ^1L_a state. Excitation at 277 nm, on the other hand, should populate the lowest vibronic levels of the $^1n\pi^*$ and ^1L_b states. The significantly longer lifetime of the ^1L_b state (750 fs) and the $^1n\pi^*$ state (>2 ps) can be explained by the barriers along the CI_{32} and CI_{16} reaction paths as discussed above. The additional decay channel, for which Ullrich et al.[13,14] have found evidence at 267 nm, possibly is the $^1\pi\sigma^*$-driven hydrogen-abstraction process.[21]

Another aspect on which we can comment on the basis of the present results is the observed solvation effect on the photophysics of adenine. Adenine in aqueous solution has a lifetime of 180 fs,[3] as compared to about 1 ps in the gas phase.[6,7] It is a well-known fact that in polar solvents $n\pi^*$ excited states are shifted to higher energy. Usually, the opposite is true for $\pi\pi^*$ states, which are shifted to the red. The reason for these trends is that $n\pi^*$ states generally are less polar than the ground state and the $\pi\pi^*$ states (cf., Table 1) and, in addition, form weaker hydrogen bonds with protic solvents than the latter. In the case of adenine, the ^1L_a state indeed is the most polar state among the lowest singlet states (see Table 1). This state is thus expected to be stabilized most in polar (and protic) solvents. The ^1L_a state correlates diabatically and in a barrierless manner to the CI_{32} conical intersection; see Figure 6b. In polar solvents, we thus can expect a photophysical behavior that is similar to the case of isolated adenine excited with a larger excess of energy, as discussed above. To explore the condensed-phase spectroscopy of adenine, additional studies are necessary, in particular the investigation of the effects of complexation with solvent molecules on the excited-state potential-energy surfaces. One of the questions which has to be investigated is how hydrogen bonding with protic solvent molecules will modify the out-of-plane deformations of the six-membered ring and the conical intersections with the ground state.

4. Conclusions

Extensive calculations of equilibrium structures, saddle points, and reaction paths on the potential-energy surfaces of the lowest excited singlet states of 9H-adenine have been performed with

(54) Nir, E.; Kleinermanns, K.; Grace, L. I.; de Vries, M. S. *J. Phys. Chem. A* **2001**, *105*, 5106.
(55) Nir, E.; Grace, L. I.; Brauer, B.; de Vries, M. S. *J. Am. Chem. Soc.* **1999**, *121*, 4896.

the CASSCF and CASPT2 methods. The excited-state equilibrium geometry is predicted to be slightly nonplanar for the $^1\pi\pi^*(^1L_b)$ state and significantly nonplanar for the $^1n\pi^*$ state. While the $^1L_b(\pi\pi^*)$ state is the lowest state in the vertical absorption spectrum of 9H-adenine, the $^1n\pi^*$ state becomes the lowest excited state at its equilibrium geometry. The structure of the conical intersection of the ^1L_b and $^1n\pi^*$ states has been determined at the CASSCF level. The $^1L_b-^1n\pi^*$ conical intersection and the strong vibronic coupling between these states provide the mechanism for a very rapid transition from the optically weakly allowed ^1L_b state to the optically nearly forbidden $^1n\pi^*$ state.

Two novel pathways that bring the S_1 and S_0 surfaces to intersection by out-of-plane deformations of the six-membered ring have been identified. The first S_1-S_0 conical intersection (CI_{32}) involves twisting of the N_3C_2 bond and results from the crossing of the diabatic ^1L_a state with the ground state. The second S_1-S_0 conical intersection (CI_{16}) involves the torsion of the N_1C_6 bond of the six-membered ring and is the result of the crossing of the diabatic $^1n\pi^*$ state with the ground state. The barriers that separate the minimum of the S_1 surface from the CI_{32} and CI_{16} conical intersections are predicted to be of the order of 0.1 eV. Both S_0-S_1 conical intersections can thus be accessed from the optically prepared vibronic levels if the excess energy on the S_1 surface is larger than about 0.1 eV. Internal conversion via out-of-plane deformations of the six-membered ring is thus, in our opinion, the dominant mechanism for the rapid radiationless deactivation of the excited singlet states of adenine. At higher energies, above about 5.0 eV, ultrafast hydrogen abstraction from the NH and NH_2 groups via repulsive $^1\pi\sigma^*$ states is a competing deactivation mechanism.

The calculated potential-energy energy profiles of the excited states along the LIIC reaction path leading to the CI_{32} conical intersection show that the ^1L_a energy is essentially repulsive along this path and crosses the potential-energy functions of the ^1L_b and $^1n\pi^*$ states on the way. This result indicates that the ^1L_a state is extremely short-lived. The excitation of the strongly allowed ^1L_a state will populate the less allowed ^1L_b and $^1n\pi^*$ states because of the conical intersections between them. The existence of a strong coupling between the ^1L_b and $^1n\pi^*$ states, as discussed above, can provide the explanation for the existence of three decay channels with lifetimes of 50 fs, 750 fs, and >2 ps, as observed by femtosecond photoelectron spectroscopy.[13,14]

This qualitative picture of the photophysics of 9H-adenine is similar to previous theoretical results[15,16,17,39] for pyrimidine bases insofar as the critical importance of out-of-plane deformations of six-membered rings of DNA bases in low-lying singlet states are highlighted. It should be mentioned, however, that these reactive pathways, which are likely to govern photophysical behavior of isolated purine bases, are possibly inactive in the Watson−Crick base pairs. The strong interbase hydrogen-bonding interactions can prevent the out-of-plane deformation of the purine bases, as shown for the guanine−cytosine base pair.[39] The effect of hydrogen bonding in base pairs apparently is too weak, on the other hand, to suppress out-of-plane distortions of the pyrimidine bases.[39]

Acknowledgment. This work has been supported by the Deutsche Forschungsgemeinschaft, the Fonds der Chemischen Industrie, and the Ministry for Science and Informatic of Poland.

Supporting Information Available: Cartesian coordinates and CASSCF canonical energies. This material is available free of charge via the Internet at http://pubs.acs.org.

JA044321C